

# Benzene-1,3-Dihydrogensulfate as a Non-Cyclic Ionophore: Selective Extraction and Transport of Metal Ions

 Amit Kumar Khandelwal,<sup>1,\*</sup>
 Poonam Hariyani,<sup>1</sup>
 Barkha Shrivastava<sup>2</sup>

<sup>1</sup> Department of Chemistry, JECRC University, Jaipur-303905, Rajasthan, India

<sup>2</sup> Department of Chemistry, JECRC College, Jaipur-302022, Rajasthan, India

\* Corresponding author's e-mail address: amitkhandelwal.aks@gmail.com

RECEIVED: March 11, 2025 \* REVISED: April 28, 2025 \* ACCEPTED: May 16, 2025

**Abstract:** This study investigates the synthesis and characterization of benzene-1,3-dihydrogensulfate, a non-cyclic ionophore for the selective extraction and transport of targeted metal ions. The synthesized ionophore demonstrated high selectivity for alkali metal ions (Na<sup>+</sup> and K<sup>+</sup>) compared to transition metals (Zn<sup>2+</sup>, Ni<sup>2+</sup>) in aqueous solutions. The observed selectivity is attributed to ion size, charge density, associated anions, coordination geometry, and the solvent medium. IR, NMR, mass spectrometry, and elemental analysis were used to establish the structure, and computer modeling shed light on the electronic characteristics. These findings suggest the potential application of this ionophore in metal separation processes, particularly for the efficient recovery of alkali metals from complex mixtures.

**Keywords:** ionophore, extraction, transport, spectrometry, computer modeling.

## INTRODUCTION

**S** ELECTIVE ion transport is a major constituent in biological systems, industrial separation processes, and environmental applications. In biological systems, it decides cellular homeostasis and nerve signal transmission processes with metabolic processes like the sodium-potassium pump<sup>[1,2]</sup> and ATP synthesis.<sup>[3]</sup> Industrially, ion transport is an essential criterion in designing selective separation technologies that recover precious metals,<sup>[4]</sup> purify water in desalination systems,<sup>[5]</sup> and facilitate environmental remedies by removing hazardous materials from wastewater.<sup>[6,7]</sup>

Ionophores are specialized molecules with the integral role of transporting ions across membranes; thus, their ability to selectively bind to certain metal ions has attracted a fair amount of attention. They have found extensive applications in metallurgical processes,<sup>[8]</sup> environmental emergency response, and biosensing technologies.<sup>[9,10]</sup> However, existing ionophores often show less selectivity, are not necessarily stable in many solvent

environments, and are very costly to manufacture.<sup>[11]</sup> Cyclic ionophores such as crown ethers, cryptands, and calixarenes received substantial attention for their well-defined binding cavities and intrinsic preorganization for cationic and anionic species.<sup>[12–14]</sup> Crown ethers, pioneered by Pedersen,<sup>[15]</sup> selectively bind alkali metal ions based on cavity size matching, and have been widely used in both biological mimetics and synthetic ion transport systems. Cryptands and calixarenes, with their more complex three-dimensional architectures, offer enhanced selectivity and tunability and have seen applications in ion sensing, extraction, and catalysis.<sup>[16–18]</sup>

Despite their advantages, cyclic ionophores also face notable limitations. Their synthesis is often labor-intensive and costly, particularly for large-scale applications. Moreover, their rigid preorganization, while beneficial for selectivity, can reduce adaptability toward different ion sizes or solvation environments. This lack of flexibility may hinder performance in variable or mixed-ion conditions, which are common in real-world applications. Furthermore, many cyclic ionophores exhibit limited

stability in non-aqueous or harsh solvent conditions, which restricts their use in industrial settings.<sup>[19]</sup>

In contrast, non-cyclic ionophores represent a promising alternative owing to their structural flexibility, synthetic accessibility, and potential for enhanced binding diversity. Although traditionally considered less selective than their cyclic counterparts, non-cyclic ionophores can adopt various conformations to accommodate a wider range of ionic radii and coordination geometries. This conformational adaptability may lead to improved performance in systems requiring multi-ion recognition or dynamic selectivity tuning.<sup>[20]</sup> Additionally, their relatively simple synthesis routes make them attractive candidates for scalable ion extraction and transport systems.

We proposed a dual approach combining experimental synthesis and computational optimization of benzene-1,3-dihydrogensulfate as a simple non-cyclic ionophore for targeted metal ions extraction and transport studies. Crown ethers, cryptands, and other cyclic ionophores<sup>[21]</sup> tend to be selective by their built-in preorganization but non-cyclic ionophores boast maximum flexibility in the aspect of ion binding, which can lead to better ion selectivity and improve transport efficiency.<sup>[22]</sup>

Here, the selectivity of the synthesized compound benzene-1,3-dihydrogensulfate toward sodium and potassium ions is examined, contrasting the extraction and transport against transition metals such as  $\text{Zn}^{2+}$  and  $\text{Ni}^{2+}$ . An analysis of pertinent parameters influencing the effectiveness will be pursued, comprising the size of the ion, charge density, and polarity of the solvent.

The computational modeling performed with Avogadro,<sup>[23]</sup> GAMESS,<sup>[24]</sup> (2020 R2) and wxMacMolPlt<sup>[25]</sup> provide an understanding of the electronic structures, binding affinities, and transport mechanisms of the synthesized ionophore. Moreover, to establish the structural identity and purity of the synthesized ionophore, experimental characterization *via* infrared (IR) spectroscopy,<sup>[26]</sup> nuclear magnetic resonance (NMR) spectroscopy,<sup>[27]</sup> mass spectrometry,<sup>[28]</sup> and elemental analysis<sup>[29]</sup> were conducted. This study's results will further contribute to designing more efficient ion-selective membranes, sensors, and industrial systems for metal recovery from impurities,<sup>[30–31]</sup> which will further enlarge the range of applications for noncyclic ionophores in liquid-liquid extraction and transport methods.

## Experimental Procedure

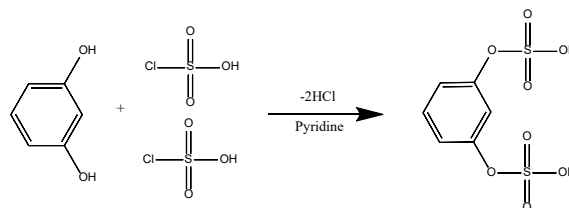
### Reagents

Reagent-grade resorcinol (CDH, 99 %), chlorosulfonic acid (Qualigens, 99 %), and pyridine (Qualigens, 98 %) chemicals were used without further purification. Analytical solvents including 1,2-Dichloroethane (Finar, 99 %) chloroform (Finar, 99.8 %) were also used without additional

purification.<sup>[32]</sup> The metal salts in the form of picrates, dinitrophenolates, and *o*-nitrophenolates ( $\text{MX}_n$ :  $\text{M}^{n+} = \text{Zn}^{2+}$ ,  $\text{Na}^+$ ,  $\text{K}^+$ ,  $\text{Ni}^{2+}$ ;  $\text{X}^- = \text{Pic}^-$ ,  $\text{Dnp}^-$ , and  $\text{Onp}^-$ ) were prepared following previously reported methods.<sup>[33]</sup>

### Synthesis of Benzene-1,3-dihydrogensulfate

The ionophore was synthesized by refluxing resorcinol (5.51 g, 0.05 mol) and chlorosulfonic acid (13.98 g, 0.12 mol) in the presence of pyridine, following the method outlined in Scheme 1.<sup>[34–35]</sup> The crude product was purified



Scheme 1. Synthesis of benzene-1,3-dihydrogensulfate.

*via* distillation, and any trace amounts of sulfuric acid were removed by treatment with  $\text{BaCO}_3$ ,<sup>[36]</sup> followed by filtration. The synthesized ionophore exhibited a yellow-brown color and a yield of 76 %. The synthesized ionophore was confirmed through IR, H-NMR, and mass spectral techniques<sup>[37]</sup> and elemental analysis.

### Computational Analysis

The effectiveness of extracting and transporting metal salts through a bulk liquid membrane (BLM)<sup>[38]</sup> system that incorporates this ionophore is affected by several physicochemical factors, such as the optimization of the ionophore and the properties of molecular orbitals. In this research, Avogadro software was utilized to optimize the ionophore (Figure 1), resulting in an energy level of 980.47 kJ/mol.

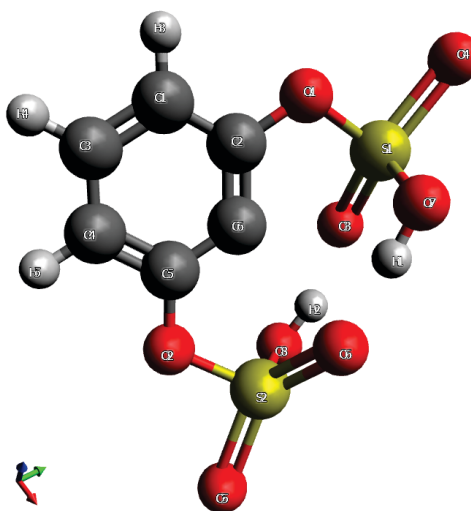


Figure 1. Optimized molecular structure of benzene-1,3-dihydrogensulfate.

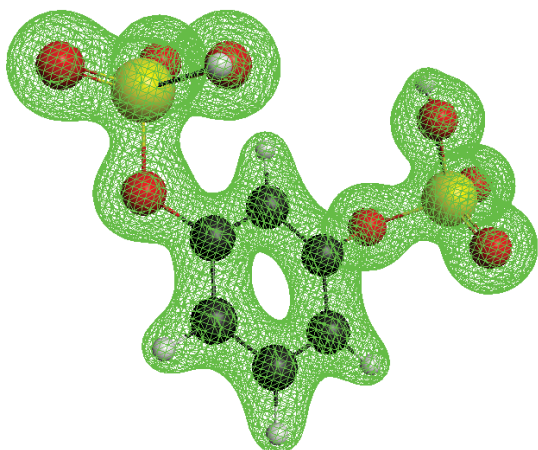


Figure 2. 3D electron density map of benzene-1,3-dihydrogen-sulfate.

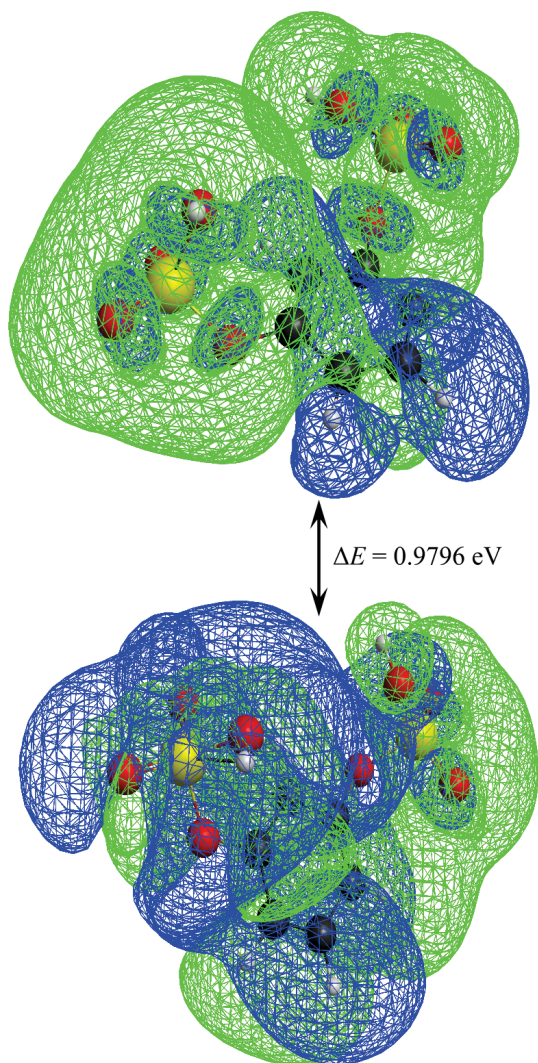


Figure 3. HOMO-LUMO visualization of benzene-1,3-dihydrogen-sulfate.

Furthermore, Computational calculations<sup>[39]</sup> were carried out using GAMESS [B3LYP/6-31G(d,p)] (see *supplementary information*), and molecular orbital visualization was performed with wxMacMolPlt. Electron density mesh (Figure 2) and HOMO-LUMO (Figure 3) show the binding efficiency, stability, and transport ability of ionophores,<sup>[40]</sup> HOMO and LUMO were found to be at  $-0.6803$  eV and  $0.2993$  eV respectively.

#### Extraction

The extraction of metal ions<sup>[41]</sup> was performed using the picrate ( $\text{Pic}^-$ ), dinitrophenolate ( $\text{Dnp}^-$ ), and *o*-nitrophenolate ( $\text{Onp}^-$ ) salts of  $\text{Na}^+$ ,  $\text{K}^+$ ,  $\text{Ni}^{2+}$ , and  $\text{Zn}^{2+}$ , in chloroform (Figure 4) and 1,2-dichloroethane (DCE) (Figure 5) to investigate the potential complexation within the pseudocyclic cavity of the synthesized ionophore.<sup>[42]</sup> The optimized metal salt concentration was  $1 \times 10^{-3}$  M, and extracted amounts were measured by the difference in concentration of ions before and after extraction in the aqueous phase. Flame photometry was used for  $\text{Na}^+$  and  $\text{K}^+$ <sup>[43]</sup> while UV-VIS spectroscopy was used for  $\text{Ni}^{2+}$  and  $\text{Zn}^{2+}$ .<sup>[44]</sup> The extraction process was conducted in triplicate, and the average extraction amount was calculated in ppm (parts per million) based on the three replicates. This ensured accuracy and reproducibility in determining the extracted metal ion concentration.

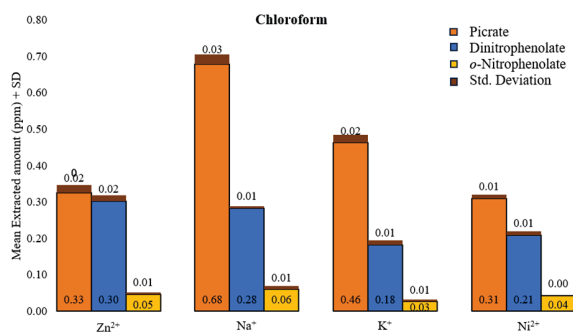


Figure 4. Extraction of metal ions in chloroform.

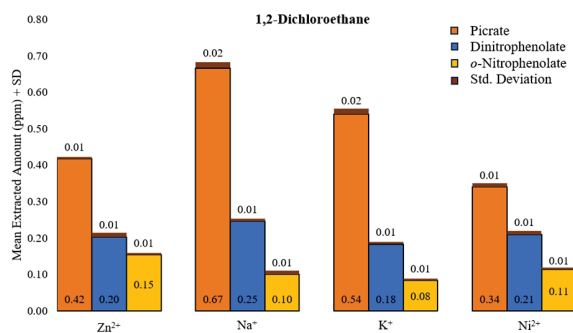


Figure 5. Extraction of metal ions in DCE.

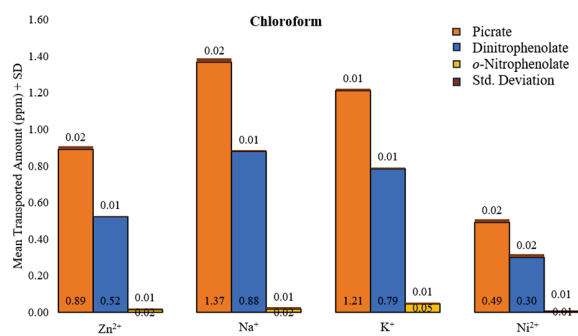


Figure 6. Transport of metal ions in chloroform.

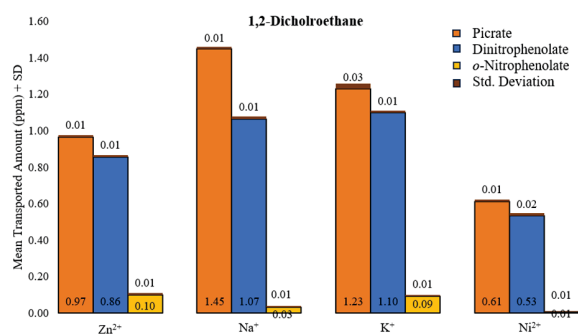


Figure 7. Transport of metal ions in DCE.

### Transport

The transport of metal ions<sup>[45]</sup> was studied using chloroform (Figure 6) and 1,2-dichloroethane (Figure 7) solvents as liquid membranes using the U-tube setup. In the U-tube, metal salts with  $1 \times 10^{-3}$  M were present in the source phase at the left side, double distilled water in the receiving phase at the right side, and both phases were separated by the respective liquid membranes having the corresponding ionophore. The U-tube was covered at both ends and placed on a magnetic stirrer. After 24 hours, the extent of decomplexation at the membrane-receiving phase interface, the amount of metal ion was evaluated in the receiving phase to assess the efficiency of transport through the ionophore. To ensure accuracy, reproducibility, and reliability, transport was also conducted in triplicate.

## Results and Discussion

### Spectral Characterization

Spectral data and elemental analysis provide a deep study of the compound and confirm the formation of a stable compound (The complete set of spectra is available in the *Supplementary Information*).

**Infrared Spectroscopy (IR).** Functional groups were confirmed using IR spectra recorded on a PerkinElmer Spectrum 10.4.00 instrument. IR ( $\text{cm}^{-1}$ ): 720.3 (aromatic C–H), 802.7 (S–OH), 1190.2 and 1060.5 (S=O), 1700.7 (C=C), 3002.1 (C–H stretching), 3300.8 (O–H).

**Nuclear Magnetic Resonance (<sup>1</sup>H NMR).** Proton chemical shifts were analyzed using a Delta2 400 MHz spectrometer in solvent  $\text{CDCl}_3$ . <sup>1</sup>H NMR ( $\delta$ , ppm):  $\delta$  7.9 (s, 1H), 9.2–9.3 (d, 2H), 8.2–8.4 (t, 1H), 12.0–12.3 (br s, 2H).

**Mass Spectrometry (MS).** The TOF Mass spectrometer was used to confirm the molecular weight. MS ( $m/z$ ): Calcd. 270.2384; Found 270.0018.

**Elemental Analysis.** The carbon, hydrogen, and sulfur contents were determined using a Thermo Fisher elemental analyzer. Elemental analysis (%): Found: C 26.58, H 2.19, S 23.8; Calculated: C 26.67, H 2.22, S 23.7.

### Computational Analysis

The optimized ionophore structure elaborates that geometry and energy states favor complexation with targeted metal ions. HOMO-LUMO energy gap of 0.9796 eV, signifying that there is a steady trade-off between stability and reactivity for effective coordination to metal ions.<sup>[46]</sup> Such moderate energy gaps allow for enhanced electron-donor and acceptor character within the ions, supporting concurrently strong and reversible metal binding that is essential for selective ion transport. Lowering the activation<sup>[47]</sup> energy promotes ion mobility throughout the phases, thus optimizing the transport kinetics in bulk liquid membrane systems. The three-dimensional mesh representing the electron density provides a clear visual representation for the emphasis on regions with electron richness, with affirmed binding sites for metal ions.<sup>[13]</sup> High electron density regions shown in green colors contribute essentially to the stabilization of metal-ion complexes and the consequential influence on selectivity.

Confirmed binding sites in the ionophore include: Oxygen atoms (O) from  $-\text{SO}_3\text{H}$  groups act as the primary coordination sites for metal ions because of their high electronegativity and ability to donate lone pairs, while sulfur (S) atoms contribute to complex stability by participating in coordination interactions. These structural and electronic confirmations further support the ionophore in prospective applications as ion-selective membranes, sensors, and metal extraction.

### Extraction and Transport

The interaction of an ionophore with metal ions decreases the effective charge of the metal ion, making it more hydrophobic and suitable for the organic solvent. This enhances the lipophilicity of the complex, allowing it to dissolve in the organic phase. The efficiency of extraction and transport is influenced by the choice of organic solvent, the anion, and the metal ion involved.<sup>[48]</sup>

The difference in polarity between 1,2-dichloroethane (DCE,  $\epsilon \sim 10.4$ ) and chloroform ( $\text{CHCl}_3$ ,  $\epsilon \sim 4.8$ ) affects the solubility of the complex. While chloroform's



lower polarity generally supports the solubility of highly lipophilic complexes like picrate, the extraction behavior with the moderately lipophilic dinitrophenolate anion reveals a more complex picture, likely involving multiple interacting factors.<sup>[49]</sup> For certain metal ions ( $\text{Zn}^{2+}$  and  $\text{Na}^+$ ), extraction with dinitrophenolate is observed to be slightly more favorable in chloroform than in the more polar DCE. In contrast, other metal ions ( $\text{K}^+$  and  $\text{Ni}^{2+}$ ) show similar extraction efficiencies with dinitrophenolate in both solvents. This suggests that factors beyond bulk solvent polarity, such as specific ion-solvent and ion-ligand interactions, significantly influence the extraction of these moderately lipophilic complexes. Additionally, the viscosity and density of the solvent play a role in diffusion and transport rates.<sup>[50]</sup>

Highly lipophilic picrate anions create stable metal complexes, promoting efficient extraction in both solvents due to significant charge delocalization. DCE has better solvating ability for polar species and may facilitate more efficient extraction of certain metal complexes. On the other hand, dinitrophenolate, with its moderate lipophilicity, exhibits varied extraction behavior, suggesting that the influence of solvent polarity on the extraction of metal-dinitrophenolate depends on the specific metal ion. This indicates that the factors, specific ion-solvent interactions, and the detailed extraction mechanism, play a significant role. *o*-nitrophenolate, being the least lipophilic, produces weak complexes, resulting in minimal extraction efficiency.<sup>[51]</sup>

Metal extraction is influenced by factors such as charge density<sup>[52]</sup> and hydration energy.<sup>[53]</sup> Ions with high charge density tend to create strong hydration shells, which decrease extraction efficiency but enhance transport. Among the metal ions studied,  $\text{Na}^+$  consistently shows higher extraction efficiencies, particularly with picrate, likely due to its smaller ionic radius and higher mobility in forming extractable ion pairs.  $\text{Na}^+$  ( $4.93 \times 10^{10} \text{ C / m}^2$ ) has a high hydration energy, making desolvation a challenging process, which can limit extraction efficiency despite favorable ion-pair formation, although transport remains efficient.  $\text{K}^+$ , with a somewhat lower charge density, shows improved extraction and transport kinetics relative to  $\text{Zn}^{2+}$  and  $\text{Ni}^{2+}$ , yet is still not as efficient as  $\text{Na}^+$ .  $\text{Zn}^{2+}$  and  $\text{Ni}^{2+}$ , possessing high charge densities and smaller ionic radii, establish strong ion-ionophore interactions, obstructing dissociation, and mobility within liquid membranes. In contrast,  $\text{Na}^+$  and  $\text{K}^+$  can undergo rapid complexation and decomplexation, which aids in efficient transport across membranes. The ligand field stabilization energy (LFSE) of  $\text{Ni}^{2+}$  results in stable complexes in the aqueous phase,<sup>[54]</sup> thereby reducing its likelihood of partitioning into the organic phase, complicating extraction, and transport.  $\text{Zn}^{2+}$ , having a lower

desolvation energy<sup>[55]</sup> compared to  $\text{Ni}^{2+}$ , can migrate more easily into the organic phase, leading to enhanced extraction efficiency.

The combination of these variables – solvent polarity, anion characteristics, and metal ion attributes – ultimately influences the overall efficacy of extraction and transport. Tables 1–4 summarize the comparative extraction and transport amounts of the mentioned metal salts (See *Supplementary Information*). This knowledge is vital for designing and optimizing liquid membrane systems to regulate metal ions in contexts such as environmental remediation.<sup>[56]</sup>

## CONCLUSION

The synthesized ionophore demonstrates a strong preference and binding capacity for  $\text{Na}^+$  and  $\text{K}^+$  ions, particularly in conjunction with picrate anions, as evidenced by both computational analyses and experimental findings. These results underscore the significance of ionophore-metal interactions for various industrial applications, environmental cleanup efforts, and metal recovery by emphasizing the roles of ion size, coordination geometry, and solvent characteristics.<sup>[57]</sup> Enhanced comprehension of binding affinities, selectivity mechanisms, and ionophore design is achieved through the integration of computational modeling and experimental synthesis, which reduces the reliance on trial-and-error methods in extractive chemistry. The synergy of these approaches facilitates the development of efficient extractants, fostering advancements in membrane-based metal extraction technologies, chemical separations, and waste management strategies. Future studies should aim to refine ionophore structures for better selectivity, create methods for scalable synthesis, and investigate alternative solvents to further boost efficiency and usability in practical applications.<sup>[58]</sup>

While this study provides valuable insights into the extraction behavior of  $\text{Zn}^{2+}$ ,  $\text{Na}^+$ ,  $\text{K}^+$ , and  $\text{Ni}^{2+}$  using picrate, dinitrophenolate, and *o*-nitrophenolate salts in two common organic solvents (chloroform and DCE), the scope remains limited to a specific set of conditions. Further research is warranted to explore a wider range of metal ions, including lanthanides, alkaline earth metals, and actinides, which may exhibit different coordination behaviors and extraction profiles. Additionally, the use of alternative solvents with varying dielectric constants and donor properties (e.g., nitrobenzene, ionic liquids, or green solvents) could provide deeper insight into solvent-solute interactions. Investigating other anionic ligands with varied electronic and steric properties would also enhance the understanding of selective metal ion transport and separation mechanisms.

**Acknowledgment.** The authors would like to acknowledge the use of GAMESS software for conducting parameter calculations, Avogadro for its assistance in molecular structure elucidation and optimization, and wxMacMolPlt for visualization purposes. We are also grateful to MNIT Jaipur for granting access to their facilities for IR, NMR, and Mass Spectrometry analyses, as well as to SAIF-IIT Bombay for their support in elemental analysis.

**Supplementary Information.** Supporting information to the paper is attached to the electronic version of the article at: <https://doi.org/10.5562/cca4167>.

PDF files with attached documents are best viewed with Adobe Acrobat Reader which is free and can be downloaded from [Adobe's web site](https://www.adobe.com/acrobat/).

## REFERENCES

- [1] S. Huang, W. Dong, X. Lin, J. Bian, *Neural Regen. Res.* **2024**, *19*, 2684–2697. <https://doi.org/10.4103/NRR.NRR-D-23-01175>
- [2] C. R. Rose, A. Verkhatsky, *Glia* **2016**, *64*, 1611–1627. <https://doi.org/10.1002/glia.22964>
- [3] M. Bonora, S. Patergnani, A. Rimessi, E. De Marchi, J. M. Suski, A. Bononi, C. Giorgi, S. Marchi, S. Missiroli, F. Poletti, M. R. Wieckowski, P. Pinton, *Purinergic Signal.* **2012**, *8*, 343–357. <https://doi.org/10.1007/s11302-012-9305-8>
- [4] S. Krishnan, N. S. Zulkapli, H. Kamyab, S. M. Taib, M. F. B. M. Din, Z. A. Majid, S. Chaiprapat, I. Kenzo, Y. Ichikawa, M. Nasrullah, S. Chelliapan, N. Othman, *Environ. Technol. Innov.* **2021**, *22*, 101525. <https://doi.org/10.1016/j.eti.2021.101525>
- [5] J. R. Werber, C. O. Osuji, M. Elimelech, *Nat. Rev. Mater.* **2016**, *1*, 16018. <https://doi.org/10.1038/natrevmats.2016.18>
- [6] B. J. Alloway in *Heavy Metals in Soils*, Vol. 22, Springer, **2013**, 3–9. [https://doi.org/10.1007/978-94-007-4470-7\\_1](https://doi.org/10.1007/978-94-007-4470-7_1)
- [7] J. P. Vareda, A. J. M. Valente, L. Durães, *Adv. Colloid Interface Sci.* **2021**, *289*, 102364. <https://doi.org/10.1016/j.cis.2021.102364>
- [8] L. Sun, C. Sun, X. Sun, *Electrochim. Acta* **2016**, *220*, 690–698. <https://doi.org/10.1016/j.electacta.2016.10.156>
- [9] B. Sharma, S. Tiwari, S. Bisht, A. Bhrdwaj, A. Nayarisseri, L. Tewari, *J. Environ. Chem. Eng.* **2023**, *11*, 109629. <https://doi.org/10.1016/j.jece.2023.109629>
- [10] M. Yonkunas, M. Kurnikova, *Front. Pharmacol.* **2015**, *6*, 1–11. <https://doi.org/10.3389/fphar.2015.00284>
- [11] P. A. Gale, J. T. Davis, R. Quesada, *Chem. Soc. Rev.* **2017**, *46*, 2497–2519. <https://doi.org/10.1039/C7CS00159B>
- [12] A. Bianchi, K. B. James, E. G. España in *Supramolecular Chemistry of Anions* (Eds.: J. M. Lehn) Wiley-VCH, **1997**, pp. 79–82.
- [13] G. W. Gokel, W. M. Leevy, *Chem. Rev.* **2005**, *105*, 667–669. <https://doi.org/10.1021/cr0200155>
- [14] C. D. Gutsche, *Calixarenes: An introduction*. Royal Soc. Chem. **2008**, 164–207. <https://doi.org/10.1039/9781847558190>
- [15] C. J. Pedersen, *J. Am. Chem. Soc.* **1967**, *89*, 7017–7036. <https://doi.org/10.1021/ja01002a035>
- [16] B. Dietrich, J. M. Lehn, J. P. Sauvage, *Tetrahed. Lett.* **1969**, *10*, 2885–2888. [https://doi.org/10.1016/S0040-4039\(01\)99235-7](https://doi.org/10.1016/S0040-4039(01)99235-7)
- [17] P. D. Beer, P. A. Gale, *Angew. Chem. Int. Ed.* **2001**, *40*, 486–516. [https://doi.org/10.1002/1521-3773\(20010202\)40:3<486::AID-ANIE486>3.0.CO;2-9](https://doi.org/10.1002/1521-3773(20010202)40:3<486::AID-ANIE486>3.0.CO;2-9)
- [18] R. M. Izatt, J. J. Christensen, *Selective Ion Exchange and Ion Pair Extraction*. Wiley-Interscience, 1978.
- [19] M. Komiyama, T. Takeuchi, T. Mukawa, H. Asanuma in *Molecular Imprinting: From Fundamentals to Applications*. Wiley-VCH, Weinheim **2004**.
- [20] C. Caltagironea, P. A. Gale, *Chem. Soc. Rev.* **2009**, *38*, 520–563. <https://doi.org/10.1039/B806422A>
- [21] F. Davis, S. P. J. Higson, *Macrocycles*, Wiley, **2011**, p. 34. <https://doi.org/10.1002/9780470980200.ch3>
- [22] A. K. Khandelwal, P. Hariyani, B. Shrivastava, *Evergreen* **2024**, *11*, 2996–3004. <https://doi.org/10.5109/7326940>
- [23] M. D. Hanwell, D. E. Curtis, D. C. Lonie, T. Vandermeersch, E. Zurek, G. R. Hutchison, *J. Cheminform.* **2012**, *4*, 1–17. <https://doi.org/10.1186/1758-2946-4-17>
- [24] G. M. J. Barca, C. Bertoni, L. Carrington, D. Datta, N. De Silva, J. E. Deustua, D. G. Fedorov, J. R. Gour, A. O. Gunina, E. Guidez, T. Harville, S. Irle, J. Ivanic, K. Kowalski, S. S. Leang, H. Li, W. L., J. J. Lutz, I. Magoulas, J. Mato, V. Mironov, H. Nakata, B. Q. Pham, P. Piecuch, D. Poole, S. R. Pruitt, A. P. Rendell, L. B. Roskop, K. Ruedenberg, T. Sattasathuchana, M. W. Schmidt, J. Shen, L. Slipchenko, M. Sosonkina, V. Sundriyal, A. Tiwari, J. L. Galvez Vallejo, B. Westheimer, M. Wloch, P. Xu, F. Zahariev, M. S. Gordon, *J. Chem. Phys.* **2020**, *152*, 154102. <https://doi.org/10.1063/5.0005188>
- [25] B. M. Bode, M. S. Gordon, *J. Mol. Graph. Model.* **1998**, *16*, 133–138. [https://doi.org/10.1016/S1093-3263\(99\)00002-9](https://doi.org/10.1016/S1093-3263(99)00002-9)
- [26] J. D. Rodriguez, D. Kim, P. Tarakeswar, J. M. Lisy, *J. Phys. Chem. A* **2010**, *114*, 1514–1520. <https://doi.org/10.1021/jp907838r>

- [27] Y. Zhang, J. Zhou, T. Yang, X. Li, Y. Zhang, Z. Huang, G. J. Mattos, N. Y. Tiuftiakov, Y. Wu, J. Gao, Y. Qin, E. Bakker, *ACS Sensors* **2024**, *9*, 6512-6519. <https://doi.org/10.1021/acssensors.4c01907>
- [28] P. J. Ducrest, S. Pfammatter, D. Stephan, G. Vogel, P. Thibault, B. Schnyder, *Sci. Rep.* **2019**, *9*, 5814. <https://doi.org/10.1038/s41598-019-42167-0>
- [29] T. A. Ali, W. H. Mahmoud, G. G. Mohamed, *Appl. Organomet. Chem.* **2019**, *33*, 1-17. <https://doi.org/10.1002/aoc.5206>
- [30] G. I. Mohammed, A. L. Saber, H. A. El-Ghamry, J. T. Althakafy, H. Alessa, *Arab. J. Chem.* **2021**, *14*, 103210. <https://doi.org/10.1016/j.arabjc.2021.103210>
- [31] S. Chen, J. Yan, J. Li, D. Lu, *Microchem. J.* **2019**, *147*, 232-238. <https://doi.org/10.1016/j.microc.2019.02.066>
- [32] Keith A. Kvenvolden and J. M. Hayes, **1969**, NASA-TM-X-1746. <https://ntrs.nasa.gov/citations/19690009624>
- [33] L. Lokwani, U. Sharma, *Main Gr. Met. Chem.* **2008**, *31*, 235-242. <https://doi.org/10.1515/MGMC.2008.31.5.235>
- [34] S. Miron, G. H. Richter, *J. Am. Chem. Soc.* **1949**, *71*, 453-455. <https://doi.org/10.1021/ja01170a022>
- [35] Norris LR III, Virginia Polytechnic Institute and State University, **1972**. <http://hdl.handle.net/10919/74621>
- [36] H. Cerfontain, N. Coenjaarts, K. K. Telder, *Recl. Des Trav. Chim. Des Pays-Bas.* **1989**, *108*, 7-13. <https://doi.org/10.1002/recl.19891080103>
- [37] M. Ragan, *Can. J. Chem.*, **1978**, *56*, 2681-2685. <https://doi.org/10.1139/v78-441>
- [38] S. H. Chang, Desalin. Water Treat. **2016**, *57*, 19785-19793. <https://doi.org/10.1080/19443994.2015.1102772>
- [39] M. W. Schmidt, K. K. Baldrige, J. A. Boatz, S. T. Elbert, M. S. Gordon, J. H. Jensen, S. Koseki, N. Matsunaga, K. A. Nguyen, S. Su, T. L. Windus, M. Dupuis, J. A. Montgomery, *J. Comput. Chem.*, **1993**, *14*, 1347-1363. <https://doi.org/10.1002/jcc.540141112>
- [40] D. M. Gil, M. E. Defonsi Lestard, O. Estévez-Hernández, J. Duque, E. Reguera, *Spectrochim. Acta Part A Mol. Biomol. Spectrosc.* **2015**, *145*, 553-562. <https://doi.org/10.1016/j.saa.2015.02.071>
- [41] P. Vaňura, E. Makrlík, *Radiochim. Acta* **2023**, *111*, 839-844. <https://doi.org/10.1515/ract-2023-0128>
- [42] H. Tsukube, in Cation Bind. by Macrocycles (Eds.: Y. Inoue, G.W. Gokel), Routledge, **2018**, pp. 492-517. <https://doi.org/10.1201/9781315138893>
- [43] P. Chavan, D. Kamble, D. Pansare, R. Shelke, M. Rai, *Asian J. Res. Chem.* **2024**, *17*, 337-343. <https://doi.org/10.52711/0974-4150.2024.00057>
- [44] F. Zhou, C. Li, H. Zhu, Y. Li, *Optik* **2019**, *182*, 58-64. <https://doi.org/10.1016/j.ijleo.2018.12.159>
- [45] P. Ajwani, L. Lokwani, U. Sharma, *Proc. Natl. Acad. Sci. India Sect. A Phys. Sci.* **2012**, *82*, 91-95. <https://doi.org/10.1007/s40010-012-0013-0>
- [46] S. Kaur, B. A. Shiekh, D. Kaur, I. Kaur, *J. Mol. Liq.* **2021**, *333*, 115954. <https://doi.org/10.1016/j.molliq.2021.115954>
- [47] S. Taniguchi, M. Aniya, *Thermochim. Acta* **2012**, *532*, 107-110. <https://doi.org/10.1016/j.tca.2011.01.018>
- [48] V. Gautam, L. Lokwani, S. Sharma, *Int. J. Innov. Res. Sci. Eng. Technol.* **2015**, *04*, 2079-2087. <https://doi.org/10.15680/IJRSET.2015.0404038>
- [49] U. Olsher, H. Feinberg, F. Frolov, G. Shoham, *Pure Appl. Chem.* **1996**, *68*, 1195-1199. <https://doi.org/10.1351/pac199668061195>
- [50] J. He, H. Fan, M. Elimelech, Y. Li, *J. Memb. Sci.* **2024**, *708*, 123055. <https://doi.org/10.1016/j.memsci.2024.123055>
- [51] M. S. Jasmin Suljagić, E. Bjelić, A. Kovačević, *Technol. Acta Sci. J. Chem. Technol.* **2022**, *15*, 47-51. <https://doi.org/10.5281/zenodo.6921068>
- [52] D. Mishra, U. Sharma, *Sep. Purif. Technol.* **2002**, *27*, 51-57. [https://doi.org/10.1016/S1383-5866\(01\)00194-0](https://doi.org/10.1016/S1383-5866(01)00194-0)
- [53] R. Lommelen, B. Onghena, K. Binnemans, *Inorg. Chem.* **2020**, *59*, 13442-13452. <https://doi.org/10.1021/acs.inorgchem.0c01821>
- [54] D. A. Johnson, P. G. Nelson, *Inorg. Chem.* **1995**, *34*, 3253-3259. <https://doi.org/10.1021/ic00116a018>
- [55] X. Cheng, Y. Zuo, Y. Zhang, X. Zhao, L. Jia, J. Zhang, X. Li, Z. Wu, J. Wang, H. Lin, *Adv. Sci.* **2024**, *11*, 2401629. <https://doi.org/10.1002/adv.202401629>
- [56] A. Kumar, A. Thakur, P. S. Panesar, *Rev. Environ. Sci. Biotech.* **2019**, *18*, 153-182. <https://doi.org/10.1007/s11157-019-09492-2>
- [57] R. Barzaga, L. Lestón-Sánchez, F. Aguilar-Galindo, O. Estévez-Hernández, S. Díaz-Tendero, *Inorg. Chem.* **2021**, *60*, 11984-12000. <https://doi.org/10.1021/acs.inorgchem.1c01068>
- [58] A. Barhoum, Y. Alhashemi, Y. M. Ahmed, M. S. Rizk, M. Bechelany, F. M. Abdel-Haleem, *Front. Bioeng. Biotechnol.* **2024**, *12*, 1397587. <https://doi.org/10.3389/fbioe.2024.1397587>